Centrifuge Study on the Runout Distance of Submarine Debris Flows

Mei Yin[1], Yi Rui[2*], Yanyi Xue[1]

[1]Dr. Mei Yin

Schofield Centre, Department of Engineering

University of Cambridge, UK.

myin0915@gmail.com

[2]Dr Yi Rui

Centre for Smart Infrastructure & Construction, Department of Engineering, University of Cambridge, UK.

yr228@cam.ac.uk

[1]Yanyi Xue

Schofield Centre, Department of Engineering

University of Cambridge, UK.

crystalxue224@gmail.com

[*] Corresponding Author: Department of Engineering, Trumpington Street, Cambridge, CB2 1PZ, UK. yr228@cam.ac.uk

Abstract

In recent years, submarine debris flow has become a central scientific topic in offshore geohazards, as more offshore and nearshore structures will be constructed in the future. In this paper, a series of mini-drum centrifuge experiments on motion of submarine debris flow, which are able to correctly reproduce the self-weight stresses and gravity dependent processes, are presented. These tests were carried out using artificial submarine clay with high water content, from 93% to 149%. And the undrained shear strength of this kind of clay was extremely low, between 81Pa and 423Pa. This feature made the debris material behave as idealistic lubricating material when it was deposited, resulting in a linear relationship between water content and runout distance of strongly coherent debris flow. On the other hand, the dilation of the flow body and hydroplaning was observed for weakly coherent debris flow, which further increased the mobility of flow body. A densimetric Froude number Fr_d was used to indicate the threshold of hydroplaning, which occurs if the Fr_d is greater than 0.2. The relationship between runout distance and water content was shown to be exponential rather than linear in this situation. Finally, two simple analytical models based on prototype debris flow under 1g condition was used to validate the experiment results, which further prove the effects of the soft marine clay on the high mobility of submarine debris flow. On the other hand, when the water content exceeded 120%, the experiment results deviated from the analytical solution due to the effects of hydroplaning.

Keywords

Submarine debris flow, centrifuge test, analytical solution, hydroplaning

1. Introduction

Submarine debris flow is a significant geomorphic process that transports submarine sediment across the continental shelf and into the deep ocean. In recent years, it has been the central scientific topic in offshore geohazards, as more offshore and nearshore structures will be constructed in the future. Especially, an increasing proportion of oil and gas is now exploited from water depth around 6m-2700m areas offshore (Erna Lange, et al. 2015). It is

therefore essential to consider the risks associated with submarine debris flows, which requires engineers to be able to predict the runout distance of submarine debris flows and the range of influence. However, a prognostic prediction of the high-mobility of debris flow is rather difficult due to the complex mechanism involved, and it is also difficult to observe directly.

To solve this problem, many lab experiments have been performed as small-scale analogues to investigate the debris slurry behaviour, dynamics and depositional structures (Mohrig et al. 1999; Marr et al. 2001; Lin and Wang 2006; Breien et al. 2007; Boylan et al. 2010; Fang et al. 2012). Mohrig et al. (1998, 1999) and Mohrig and Marr (2003) carried out several laboratory experiments on the relative mobility of subaqueous and subaerial debris flows and concluded that hydroplaning cause the farther runout distance for subaqueous as compared to subaerial debris flows. Similar results were reported by Ilstad et al. (2004a, b), which indicated that the low bed friction is due to the hydroplaning of the subaqueous debris flow front. These researches were designed to explain the phenomena of long runout distance for subaqueous debris flows. However, it should be noted that geotechnical materials such as soil and rock have non-linear mechanical properties that depend on the effective confining stress and stress history, and hence a scaled-down physical model, under 1g conditions, will not be a strict representative of its geotechnical prototype (Wang, 2012). To mitigate this problem, centrifuge tests, which can apply centrifugal acceleration to correctly reproduce the full scale self weight stresses and gravity dependent processes in the model, is more appropriate for the investigation of the submarine debris flow behaviour. In order to preserve the stress-strain behaviour of prototype, a reduced-scale centrifuge model of dimensions n times smaller is used to simulate the full-scale problem under an centrifuge acceleration n times the gravity (Taylor 1995). But only a limited number of experiments have been carried out on submarine debris flows in centrifuges due to their technical complexity. Boylan et al. (2010) used drum centrifuge to model the runout of submarine debris flows triggered from an intact block of clay along a model seabed. Gue (2010) conducted centrifuge experiments on submarine debris flow and a new scaling law involving submarine debris flows was adopted. Using similar tests, Acosta et al. (2017) studied on the mechanism and parameters involved in the generation of hydroplaning during the mobility of debris flow on very gentle slopes. Wang (2017) investigated the evolution of the sediment concentration during the propagation of submarine debris flow by centrifuge tests. However, the study on the runout of debris flows in these researches were still rudimentary.

This paper presents a series of mini-drum centrifuge tests to simulate the runout distance of submarine debris flow between the source area and the final deposit. The main aim of this study is to reveal the mechanisms involved in the extraordinary mobility of submarine debris flow under the similar magnitude of soil stress and driving force with the actual geomorphic events. These tests were carried out using soil samples with a large variation in water content, from 93% to 149%, which corresponds with the changes in flow behaviour from strongly coherent to weakly coherent. The experiment results were then validated by a simple analytical model based on prototype debris flow under 1g condition.

2. Experimental details and procedures

2.1. Centrifuge apparatus

A mini-drum centrifuge was chosen for the physical modelling of submarine debris flow because of its flexibility in allowing debris materials to move freely within the circular ring channel. The mini-drum centrifuge at Schofield Centre of Cambridge University is the Mk II mini-drum, manufactured by Andrew N. Schofield & Associates (ANS&A), and has been in operation since 1995.

Figure 1. The mini-drum Centrifuge

Figure 1 portrays the mini-drum Centrifuge setup at the Schofield Centre Cambridge. The base of the ring channel has a radius of 500 mm, measured from the central shaft. It can reach 636g when the centrifuge spins at a maximum speed of 1067 rpm, where g is the gravity acceleration (9.81 m/s^2). The centrifuge has a central pivot which allows a 90^0 rotation of the channel axis from the vertical to the horizontal position. This permits a model package to be prepared in a convenient position inside the channel before spinning, and then switched to the vertical position for spinning. Water is supplied directly to the base of the ring channel in-flight though the inlet pipe. The water level in the ring channel can be varied using an adjustable stand pipe operated though an air motor, and the same apparatus can be used to drain the water after test finished. The features of the mini-drum Centrifuge are presented in more detail in Barker (1998).

2.2. Centrifuge model set-up and geometry

In order to mount the soil sample and instrumentations within the ring channel, two steel boxes was built, as shown in Figure 2. Each box was divided into two compartments: one containing the slope and soil sample, and the other equipped with the cameras. The two compartments were separated by a watertight glass partition allowing a side-view of the sliding and deposition of submarine debris flow. The channel bed consists of two sections with an average of 3^0 slope installed in two boxes. Each box subtended a central angle of 60^0, corresponding to the arc length of 1.04 m (0.52 m×2). These boxes were clamped to the ring channel and could be removed after tests.

Figure 2. Experiment set-up

In the real event, submarine debris flows may be triggered by various reasons such as an earthquake, a tsunami or a submarine volcanic activity. In this experiment, the landslide flow was triggered by piston pushing, as shown in Figure 3. The piston was activated by an air pressure pipe. And a mental protecting gate was used to protect the soil block from collapse before the piston triggered.

Figure 3. The schematic diagram of trigger system

2.3. Instrumentations

In order to monitor the submarine debris flow behaviour, the motion of the sliding debris was captured using high speed digital cameras from the side and top of the channel as shown in Figure 2. Events in the slope compartment during the tests were recorded by three digital cameras, one of which was a MotionBLITZ EoSens high-speed camera installed at the centre of the mini-drum centrifuge. A mirror was specifically made and placed on the slope compartment of Box 1, so that the side view of the flow runout could be reflected to the camera. The second camera used in the experiments was a GoPro Hero4. The miniature camera came with a waterproof case, which allowed it to be put safely in the camera compartment to catch the side view of the flow runout. To enable remote monitoring and operation, the camera was connected to Wi-Fi. The third camera used to monitor the plan view of flow runout was a Pentax Optio W10 digital camera, which was also dustproof and waterproof.

2.4. Experimental Procedures

The procedure for each test is summarized as follows:

(a) The slurry was prepared separately outside of the mini-drum centrifuge. Mixed the Kaolin clay powder and fresh water manually to achieve the required soil sample. Carried out fall cone test to measure the undrained shear strength of soil samples.

(b) Ensured that the test box in the mini-drum centrifuge was completely clear and that the watertight glass partition was clean and polished. Sandpaper was attached to the slope bed to prevent slippage.

(c) Two scales were pasted perpendicular and parallel to the slope, to measure the height and depth of the sliding debris. After model packages clamped in the mini-drum, installed the other instrumentations such as cameras. Set up the three cameras to record the side view as well as the plan view of sliding landslide.

(d) Continuous stirring was carried out before centrifuge test to ensure a homogenous mixture. Pour the soil sample into the channel of Box 1 with a 50 mm high, 50mm long and 130mm wide gap between the pushing gate and the protecting plate. The air pressure and piston were connected by a pipe before testing.

(e) Once everything was in place, the safety cover of mini-drum centrifuge was installed. The data acquisition system was switched on before spinning the centrifuge.

(f) When the experiments were then ready to be carried out, began to spin the centrifuge, The mini-drum centrifuge spun up to 10g very slowly to allow water introduced in the very early times. Once the water had steadily risen to the top of the soil sample, spin up the model progressively to 50g level. Each experiment took about half an hour to spin up to this desired acceleration level.

(g) Feed water continuously to maintain a constant water level in the channel. This could be confirmed by the side views captured by cameras. The overflow water was drained off from the ring channel.

(h) Open the high pressure pump connected to the piston to trigger the debris flow as long as the centrifuge was spinning steadily.

(i) After each test, water in the ring channel was slowly drained off while the centrifuge was still spinning. The speed of the centrifuge was lowered down progressively. Take the records from three cameras to measure flow distances again time after each test. Measured the depth and length of the deposit.

(j) The experiments were carried out for different water content levels with same acceleration level of 50g .

3. Undrained shear strength of marine clay

The triggering of submarine debris flows vary according to both the geomechanical attributes of debris material, and transient environmental changes affecting the submarine environment. Common to most of these cases is a change in the downslope driving stress such that it exceeds the basal friction to resist the flow movement. Therefore, the undrained shear strength of debris material plays an essential role in this geomorphic process. In this study, the marine clay was assumed to form the seafloor slope material. Common to most but not all cases, the marine clay near seabed have extremely high water content. For example, the water content of Ariake clay samples collected from Fukodomi town, Saga, Japan was about 130% (Miura et al., 2001). The water content of Muar clay from the west coast of Peninsular Malaysia reached about 100% (Indraratna et al. (1992). Natural water Content of marine clay from Kakinada Sea Coast, India was 96% (Rao et al., 2009). Hence, a series of centrifuge tests were performed on ten different Kaolin clay samples with water contents ranging from 93% to 149% in a 50g environment, considering the varied behaviour of submarine debris flow with different water contents. In this research, a conventional fall cone with cone angle of 30^0 and mass of 80g was initially used to measure the undrained shear strength of Kaolin clay. However, when the soil strength was less than 400Pa, the cone penetration exceeded the height of the cone (30 mm). It indicated that the measurement range was greater than the strength range of interest for soft marine clays with high water contents in surficial deposits on the seabed. Hence, two light aluminium cones with the same geometry with masses of 20 g and 13.6g were developed respectively. This enabled shear strengths down to 68Pa to be

measured accurately. The constant geometric shape of the different cones avoided differences in the remoulding effects during the test, as shown in Figure 4.

Figure 4. Three different cones used in the research

Hansbo (1957) expressed the shear strength function of fall cone dynamic penetration depth h in millimetres, as:

$$s_u = \frac{KQ}{h^2} \quad (1)$$

where Q is the weight of the cone, K is the fall cone factor, dependent on the cone angle α ($K = \frac{g}{\pi}\cos^2\frac{\alpha}{2}\cot\frac{\alpha}{2}$). On the other hand, according to British standard BS 1377 (BSI 1990), the shear strength is 1.7 kPa at the liquid limit when an 80 g cone penetrates by 20 mm. Therefore, the undrained shear strength tested by cones with the same apex angle (30^0) and mass (80g) can be written in the terms of penetration depth as:

$$s_u = \left(\frac{20}{h}\right)^2 \times 1.7\text{kPa} \quad (2)$$

Fall cone factor K is constant for cones with the same apex angle. Therefore, combining Equation (1) into Equation (2) gives the undrained shear strength equation for cones of 20g and 13.6g, respectively:

for 20g cone: $$s_u = \left(\frac{10}{h}\right)^2 \times 1.7\text{kPa} \quad (3)$$

for 13.6g cone: $$s_u = \left(\frac{8.25}{h}\right)^2 \times 1.7\text{kPa} \quad (4)$$

The undrained shear strength of soil samples tested by fall cone test is listed in Table 1.

Table 1. Clay slurries used in centrifuge test

4. Experiment results and discussion

4.1. Debris flow behaviour

Water content ranging from solid to liquid slurries was used to investigate how the flow behaviour varied in response to changing water content. According to other studies (Hampton, 1972; Marr et al. 2001; Ilstad et al. 2004a, b), the debris flow behaviour of submarine

landslide is dependent on the extent of erosion, break-up and water-entrainment at the flow head under given dynamic stresses. Marr et al. (2001) and Ilstad et al. (2004a, b) divided submarine landslide into weakly gravity flow and strongly coherent flow. Weakly coherent debris flows generate substantial turbidity currents and the flow head may break-up into a turbulent suspension. Strongly coherent flows experience limited erosion and break-up, and the interface between the debris flow and the overlying dilute turbidity current is very clear. Those two kinds of debris flow were also observed in this study.

The plan view of the debris flows (93 wt.%, 106 wt.%, 124 wt.% and 133 wt.%) are presented in Figures 5. The interval of each picture for different debris flow is 0.33s. The debris flows with low water content (93 wt.%, 106 wt.%) showed an clear and well defined flow head, due to the relatively high soil strength that was able to resist the dynamic stresses around the debris flow head. These two cases can be considered to be strongly coherent flows. On the other hand, the flow speed was very low, with final runout distance of 25cm and 35cm respectively. This was because of the shear strength which make the kinetic energy gained during the initial fall dissipate rapidly. Flow behaviour seemed to change gradually as we increased the water content. When the water content of debris material increased to 124% and 133%, the debris flow showed a moderately dilated turbidity current when it flowed down the slope with a clear tendency for head erosion and break-up. And both the flow speed and runout distance were much larger compared the upper 2 cases (93 wt.%, 106 wt.%). In this series of centrifuge experiments, the occurrence of erosion and break-up was first observed when the water content increased to 121%, and hence the transition between weakly and strongly coherent flows lied at the water content between 113% and 121%.

(a) water content: 93%
(b) water content: 106%
(c) water content: 124%
(c) water content: 133%

Figure 5. Plan view of the flow with different water content

The side view of submarine landslide flows with various water contents is shown in Figure 6. In order to compare the shapes of flow head for different submarine debris flows, Figure 6 captures the side views when these debris flows travelled a distance of 10cm (left) and 15cm (right). There was no distinct turbulent current along the slope (Figure 6a & b), which meant that no substantial water intruded the body of debris flow during the motion of debris flow.

The flow heights in Figure 6(a) & (b) were approximately 1 cm. It also can be seen that the previously deposited body of static sediment allowed the sliding debris to ramp up over it, creating a smooth and lubricating layer between slope bed and debris flow. The final deposit was shown thickest near the gate and thins down the slope. The flow behaviours shown in Figure 6(c) & (d) are quite different from those in Figure 6(a) & (b). The shear stress generated along the upper surface of the head resulted in erosion and entrainment of water into flow body. And hence the upper part of flow bodies were transformed into turbidity currents. In these two cases, it became difficult to distinguish the main debris flow and the overlying turbidity current, especially in the frontal zone. The thicknesses of the flow heads (include the turbidity currents) increased significantly. It was also found that the thicker flow head was followed by a thinly stretched flow body for these two cases. This was due to the difference in the speed of sliding debris along slope. Comparison between samples with various water contents showed that the thickness of the turbulent currents increased with the water content. This was because the higher water content was associated with a lower undrained shear strength, which meant that water eroded into the flow more easily. On the other hand, Figure 6(c) & (d) showed the dynamic pressure flow head caused the flow head uplift and detach slightly from the bed, which permitted the intrusion of a thin layer of lubricating water underneath, which would discussed later on. This in turn can cause a further reduction in the basal resistance.

(a) Water content: 93%

(b) Water content: 106 %

(c) Water content: 124%

(d) Water content: 133%

Figure 6. Side view of submarine landslide flows with various water contents

4.2. Occurrence of hydroplaning

If the debris flow speed is high enough, a layer of water would intrude underneath the front of debirs flow and therefore uplifts the flow head. This phenomena of an uplifted flow head is called ‘hydroplaning’ (Mohrig, et al., 1998; De Blasio, et al., 2004; Ilstad, et al., 2004b).

According to the side view of debris flow captured by the camera, there was no hydroplaning occurring for strongly coherent flow. For weakly coherent flow (water content > 120%), the water intrusion underneath the flow body was observed, highlighted by a dotted circle in Figure 6. On the other hand, the densimetric Froude number Fr_d was introduced to further identify the happening of hydroplaning. The threshold of hydroplaning depends on whether the stagnation pressure applied on debris flow head is large enough to penetrate into the interface between the bed and the debris. From Bernoulli's principle, the stagnation pressure is given by (Mohrig, et al., 1998; De Blasio, et.al, 2004):

$$P = \frac{1}{2} \rho_w U^2 \tag{5}$$

where ρ_w is the water density and U is the velocity of debris flow parallel to the sea floor,

According to Mohrig (1998), the balance between stagnation pressure and can be used as an indicator of the onset of hydroplaning. Hence, Mohrig (1998) presented a densimetric Froude number, Fr_d, as the indicator:

$$Fr_d = \frac{U}{\sqrt{\left(\frac{\rho_d}{\rho} - 1\right) g h_d \cos\theta}} \tag{6}$$

where ρ_d is the density of debris slurry, as listed in Table 1, ρ_w is the density of water, h_d is the thickness of the debris flow head, which was measured by the debris deposits after each test, θ is the slope angle and g is the centrifuge acceleration.

By using Equation (6), Fr_d for different water content can be calculated as shown in Figure 7. The Fr_d increased exponentially with the water content. Mohrig (1998) and Yin & Rui (2017) presented a range of Fr_d values of 0.3 to 0.4 for the onset of hydroplaning under 1g condition. In this series of centrifuge tests, the debris flows with water content of 121% and 124% have Fr_d values in the range of 0.2 to 0.3, in accordance with the phenomenon of water intrusion underneath the flow body as shown in Figure 6. Hence, it can be concluded that the threshold value of Fr_d roughly about 0.2, slightly lower than the value under 1d condition. This difference may be caused by the effects of turbulent flow, which leaded to the decrease in the depth of flow body.

Figure 7. Values of the densimetric Froude number Fr_d

4.3. Runout distance

Figure 8 shows the flow distance against time. The debris flow at the very beginning was disturbed due to the effects of the pushing mechanisms. Hence, 0.3s was selected as the initial time for data analysis. The flow distance profiles were determined from sequences of images during steady flow. For each case, the velocities (the gradient of each curve) decreased after 0.3s and finally tended to reduce to 0. Common to most but not all cases, the debris flow with a higher water content had a higher initial speed and larger runout distance. The motion of the debris flow with the lowest water content (93%) only lasted for less than 2 seconds, and the final runout distance was only about 23cm. However, when the water content increased to 149%, the debris flow reached the end of channel after 1.5s, and hence the runout distance of this case was not captured. This phenomenon indicated that water content had very large effects on the mobility of submarine debris flow.

Figure 8. Flow distance against time for flows with various water contents

Figure 9 shows the final runout distance against the various water contents. The relationship between the water content and runout distance fits well with a linear trend for the low water content cases ($R^2 = 0.99$). However, it could be found that the runout distance of flow with water content higher than 120% increased exponentially with the water content ($R^2 = 0.99$). This result indicated that the mechanisms of high motion of debris flow were different between strongly coherent flow and weakly coherent flow. For strongly coherent flow, the mobility of debris flow was mainly dependent on the extremely low undrained shear strength of marine clay. For weakly coherent flow, the mobility was affected by two other factors. The first was the undrained shear strength of the debris material not high enough to resist the water entrainment. In that case the behaviour of debris flow transmitted from strongly coherent to weakly coherent flow, which decreased the dynamic stresses applied on the flow head. Hence, the debris flow showed higher mobility. The second factor was the hydroplaning. During the motion of debris flow, the flow head lifted off the slope bed a little bit, and water intruded further beneath the flow body when the flow speed increased, causing a water layer to exist between the flow body and the slope bed, which in turn caused a further reduction in the basal resistance.

Figure 9. Relationship between flow initial water content (up to 133%) and flow distance

5 Scaling law

The principle of centrifuge modelling is to simulate the behaviour of a prototype in a small-scale model subjected to acceleration of magnitude many times the earth's gravity. With this technique, gravity-dependent processes, like submarine landslide, can be correctly reproduced, and observations from small-scale centrifuge models can be related directly to with the full-scale prototype situation using well-established scaling laws (Taylor, 1995). Hence, scaling aspects must be considered first when performing the centrifuge experiments. In this study, dynamic similarity is obtained by ensuring equality of the dimensionless numbers. The Froude number Fr, the Reynolds number Re and a dimensionless yield strength parameter $\widehat{s_u}$ are defined by:

$$\mathrm{Fr_d} = \frac{\mathrm{U}}{\sqrt{\left(\frac{\rho_d}{\rho_w}-1\right)\mathrm{g}h_d\cos\theta}} \tag{7}$$

$$\mathrm{Re} = \frac{\rho_d \mathrm{UL}}{\mu} \tag{8}$$

$$\widehat{s_u} = \frac{\tau_w}{\rho_d U^2} \tag{9}$$

where μ represents the viscosity of the debris flow, L is the travelled length, τ_w is the shear strength.

In performing similarity analysis, we assumed that $(\rho_w)_P = (\rho_w)_M$ and $(\rho_d)_P = (\rho_d)_M$. Considering centrifuge acceleration, $(g)_P \times N = (g)_M$. In addition, the application similarity in Froude number, Reynolds number and dimensionless yield strength yield the results as shown in Table 2.

Table 2. Summary of centrifuge modelling scaling law

It should be noted that the scaly of real submarine debris flows may be very large while the scaled model in 1 g test environment is relatively small, hence the soil stresses in such condition is also small and may not represent the real situations. But with centrifuge modelling, self-weight stresses and gravity dependent processes are able to be correctly

reproduced and observations from small scale models can be related to the full scale prototype situation using appropriate scaling laws. Based on the scaling law listed in Table 2, the horizontal movement would have scaled at N times of the model. Hence the largest runout distance of prototype flow could reach more than 50m in this study. And the prototype flow height was approximately about 0.2~2.0m. Ideally this gave the similar magnitude of soil stress with the real submarine landslides. On the other hand, according to Table 2, the flow velocity of a prototype scaled at 1 times of the model. The very low initial flow velocity (0.1~0.6m/s) leaded to a quite large runout distance, which demonstrated the extraordinary mobility of debris flow in this series of centrifuge experiments.

The mechanism of high mobility of the debris was explained in Figure 10. During the motion of submarine debris flow, the basal shear force was dominated by cohesion rather than Coulomb friction in undrained condition. Hence, the artificial debris flow always had very low basal shear force even under large vertical loading in the real event. This feature made the marine clay behave as idealistic lubricating material when it is deposited, allowing the sliding debris flow to ramp up over it easily. That is why the coherent debris flow still had a very high mobility even without hydroplaning happening. On the other hand, centrifuge tests revealed that the artificial submarine debris flow with high water content tended to form a thin water layer underneath the flow head which acted as another natural lubricant. This was why the runout distance increased exponentially with the water content when the hydroplaning happened. In addition, with the water entrainment, the submarine debris flow transmitted from strongly coherent to weakly coherent flow, which decreased the dynamic stresses and hence further increased the mobility of debris flow.

Figure 10. Mechanisms of high mobility of submarine debris flow

6 Fluid model

Once a debris flow is generated, the velocity of the flowing mass is considered to be such that the flowing material remains under undrained conditions. In such cases, considering the high rate of movement, the phenomenon is best described by means of fluid mechanics rather than soil mechanics (Locat and Lee, 2005). The constitutive behaviour of a fluid in motion is

generally described by Bingham model, which assumes a linear variation of the shear stress with shear strain, once the yield stress is exceeded (Johnson, 1970; Coussot, 1997)

$$\tau_w = \tau_y + \mu \frac{\partial U}{\partial y} \tag{10}$$

where y is the coordinate perpendicular to the sea floor.

The driving forces acting on the sliding debris are proportional to the gravitational acceleration component parallel to the slope bed. Meanwhile, opposing the driving forces are the friction with the slope bed and the drag force due to the surrounding fluid caused by the stagnation pressure. However, when the hydroplaning happens, it was difficult to distinguish the main debris flow and the overlying turbidity current. Hence, to determine the τ_w became a complex task. To avoid this problem, hydroplaning was not considered in the calculation of this study, and τ_w was substituted by the undrained shear strength of debris slurry for simplification. Based on the assumptions discussed above, a simplified equation of motion for the submarine debris flow is given by

$$\frac{dU}{dt} \approx -\frac{\tau_y}{h_d \rho_d} + \frac{(\rho_d - \rho_w) g \cdot \sin\theta}{\rho_d} - \frac{1}{2} \frac{\rho_w}{L_d \cdot \rho_d} U^2 \tag{11}$$

where ρ_d is the density of debris slurry, h_d is the depth of moving debris flow, θ is the slope angle of sea floor, L_d is the length of sliding debris, D_w is the thickness of this water layer and τ_y is the undrained shear strength of marine clay. If hydroplaning happens, τ_y should be replaced by the shear stress exerted by the water underneath the moving debris.

On the other hand, if the soft marine clay didn't exist, the equation listed above no longer applies. For example, the seafloor material are composed of sand or rock fragments. In this case, the shear strength at the bottom layer of debris flow follows the coulomb friction model:

$$\tau_w = (\rho_d - \rho_w) g h_d \cos\theta \cdot \tan\alpha \tag{12}$$

where α is the friction angle.

And hence Equation 11 can be rewritten as,

$$\frac{dU}{dt} \approx -\frac{(\rho_d - \rho_w) g \cos\theta \cdot \tan\alpha}{\rho_d} + \frac{(\rho_d - \rho_w) g \cdot \sin\theta}{\rho_d} - \frac{1}{2} \frac{\rho_w}{L_d \cdot \rho_d} U^2 \tag{13}$$

In order to estimate the effect of the soft marine clay on the mobility of submarine debris flow, both of the two models were calculated based on prototype debris flow under 1g condition. According to the experiment results and scaling law, several parameters was

determined. The length of sliding debris $L_d = 2.5m$. The saturated density of debris slurry was listed in Table 1. The friction angle is assumed as 30 º, which is a typical value for sand. The depth and initial velocity of moving debris flow used the observed average value for each case.

Figure 11 shows the calculated runout distance with varying water content. The run-out distance of sand debris flow was very small, less than 0.1m. This is due to the large friction, which is proportional to height of debris flow. However, the undrained shear strength is always extremely low even for these large scale submarine debris flow because of the low permeability nature of marine clay. The analytical solution of clay were close to the experiment results when hydroplaning was not occurring, which demonstrated the ability of the analytical solution to predict the runout distance of a submarine landslide to a reasonable level of accuracy. However, when the water content exceeded 120%, the experiment results deviated from the calculated value due to hydroplaning not considered in the analytical solution. The difference was about 10m when the water content increased to 139%, which further demonstrated the large effects of hydroplaning on the mobility and final runout distance. Hence, the fluid model can be used for strongly coherent flow only.

Another aspect worth mentioning is the fact that the influence of hydroplaning on the basal friction is related to water content levels, altering the values of fluid pressure, normal stress and densimetric Froude number. According to Equation 11, while considering hydroplaning, that is, the basal shear strength is dependent on the properties of water, not the debris material. In the frictional regime of granular flow theory, grains move slowly and dissipate energy through long-lasting, frictional contacts. The dissipative stress is the shear strength exerted by the water underneath the moving debris when the hydroplaning happens. Hence, once the hydroplaning happens, the variation in the mobility of the debris flow with different water content levels should be limited. However, results evidenced the occurrence of hydroplaning when the water content level of clay is higher (water content of 149%), situation in which the debris flow behaves much more mobile than other cases (water content of 121% & 124%). Hence, this phenomenon can not be explained well by the frictional theory. However, this can be explained by the fact that particle collisions also generate a dispersive normal stress or pressure. When the water intrude underneath the debris flow, the frequency of collisions between soil particles and slope bed decreases. Therefore, the total kinetic energy of the system decreases more slowly, resulting in an increase in the mobility of submarine debris

flow. In addition, this frequency of inelastic collisions is proportional to the ratio of soil to water. For the debris flow with higher water content, it means less soil particles suspended in the water and hence less chance of the collision. Therefore, the collisional theory can explain the effects of hydroplaning on the high mobility of submarine debris flow very well.

Figure 11. Calculated runout distance with varying water content

7. Conclusions

A series of mini-drum centrifuge experiments on motion of submarine debris flow are presented in this paper. These tests were carried out using debris flows with a large variation in water content, from 93% to 149%. According to the flow characteristics observed in the tests, submarine debris flows could be divided to strongly coherent flows and weakly coherent flows. The difference of these two kinds of flow depends on whether the shear strength of the debris material is high enough to prevent the intrusion of ambient water. In this series of tests, the flow behaviour transformed from strongly coherent flow to weakly coherent flow at a water content of about 120%. A simple linear relationship was proposed between the water content and the final runout distance of the debris flow. Through the linear relationship it was possible to estimate the runout distance at a given water content (below 120%). Once the water content was over 120%, the final runout distance of submarine debris flow increased sharply, and this relationship between runout distance and water content was believed to be exponential rather than linear. In addition, the hydroplaning occurs when the front of flow body was lifted up by the stagnation pressure. A densimetric Froude number Fr_d was used to indicate the threshold of hydroplaning, which occurs if the Fr_d is greater than 0.2. This threshold value of Fr_d is a little lower than the value proposed by Mohrig (1998) and Yin & Rui (2017), because of the effects of turbulent flow.

The traditional scaling law was proved to apply in the centrifuge test of submarine debris flow, due to the similarity in Froude number, Reynolds number and dimensionless yield strength. Using this scaling law the observations from small-scale centrifuge models were related directly to the full-scale prototype situation. Accordingly, two simple analytical models based on prototype debris flow under 1g condition are used to validate the experiment

results. With the coulomb friction model, the submarine debris flow showed an extremely low mobility. But the analytical solution considering the existence of the marine clay matches the experiment results quite well. A linear relationship between runout distance and water content was observed in both analytical and experiment results. It proves that the shear resistance was always very low during the sliding process, even under large vertical loading, due to the low permeability nature of marine clay. This feature made the marine clay with high water content behaved as idealistic lubricating material when it was deposited, allowing the strongly-coherent debris flow to ramp up over it easily. On the other hand, hydroplaning decreased the basal friction, which caused a further reduction in the basal resistance. However, experiment results from high water content debris flow showed that the effects of hydroplaning on the flow mobility increase with water content level. This phenomenon can be explained well by the collisional theory. The frequency of inelastic collisions is proportional to the ratio of soil to water. When water content increases, the chance of inelastic collision between suspended soil particles and slope bed decrease, and hence the water content still plays an important role for the mobility of debris flow with the occurrence of hydroplaning.

Acknowledgement

This research work is part of the activities of the Schofield Centre at University of Cambridge. The work presented in the paper is part of the Modelling of Mudslide Runout Project which was a collaborative project between University of Cambridge and BP.

We thank Dr. Stuart Haigh, (University of Cambridge) and Professor Kenichi Soga, (UC Berkeley) for comments that greatly improved the research results. We would also like to show our gratitude to Dr. Paul Dimmock (BP) for fully supported this project and sharing his pearls of wisdom with us during the collaboration.

Reference

Acosta, E. A., Tibana, S., de Almeida, M. D. S. S., & Saboya, F. (2017). Centrifuge modeling of hydroplaning in submarine slopes. *Ocean Engineering*, 129, 451-458.

Barker, H.R. (1998). Physical Modelling of Construction Processes in the Mini-Drum Centrifuge. *PhD Thesis*, University of Cambridge.

Boylan, N., Gaudin, C., White, D. J., & Randolph, M. F. (2010). Modelling of submarine slides in the geotechnical centrifuge. In *Proceedings of 7th International Conference on Physical Modelling in Geotechnics*, Zurich, Switzerland (pp. 1095-1100).

Breien, H., Pagliardi, M., Blasio, F., Issler, D., & Elverhшi, A. (2007). Experimental studies of subaqueous vs. subaerial debris flows–velocity characteristics as a function of the ambient fluid. *Submarine Mass Movements and Their Consequences*, pp. 101--110.

British Standard 1377. (1990). Methods of Test for Soils for Civil Engineering Purposes. *British Standards Institution*, London.

Coussot, P. (1997). *Mudflow Rheology and Dynamics*. Balkema, Rotterdam.

De Blasio, F.V., Engvik, L., Harbitz, C., Elverhøi, A. (2004). Hydroplaning and submarine debris flows. *Journal of Geophysical Research*, 109.

Erna Lange, Sven Petersen, Lars Rüpke, Emanuel Söding, Klaus Wallmann (2015) Oil and gas from the sea. World ocean review.

Fang, H., Cui, P., Pei, L. Z., & Zhou, X. J. (2012). Model testing on rainfall-induced landslide of loose soil in Wenchuan earthquake region. *Natural Hazards and Earth System Sciences*, 12(3), 527-533.

Gue, C. S., Soga, K., Bolton, M., & Thusyanthan, N. I. (2010). Centrifuge modelling of submarine landslide flows. *7th Int. Conf. on Physical Modelling in Geotechnics* (ICPMG), Zurich.

Hampton, M. A. (1972). The role of subaqueous debris flow in generating turbidity currents. *Journal of Sedimentary Research*, 42(4).

Hansbo, S. (1957). A new approach to the determination of the shear strength of clay by the fall-cone test. Royal Swedish Geotechnical Institute Proc., *Royal Swedish Geotechnical Institute*, Stockholm, 14, 7–47.

Ilstad, T., Marr, J., Elverhri, A., & Harbitz, C. (2004a). Laboratory studies of subaqueous debris flows by measurements of pore-fluid pressure and total stress. *Marine Geology*, 213(1-4), pp. 403--414.

Ilstad, T., Elverhri, A., Issler, D., & Marr, J. (2004b). Subaqueous debris flow behaviour and its dependence on the sand/clay ratio: a laboratory study using particle tracking. *Marine Geology* 213(1-4), pp. 415--438.

Indraratna B., Balasubramaniam A.S. and Balachandran S. 1992 Performance of test embankment constructed to failure on soft marine clay. Journal of Geotechnical Engineering 118 12-43

Johnson, A.M., 1970. *Physical Processes in Geology*. Freeman Cooper, San Francisco, CA.

Lin, M. L., & Wang, K. L. (2006). Seismic slope behavior in a large-scale shaking table model test. *Engineering Geology*, 86(2), 118-133.

Locat, J., & Lee, H. (2005). Subaqueous debris flows, Chapter 9. Mathias, Hungr (Eds.), *Debris-flows Hazards and Related Phenomena*, Springer, pp. 203-245.

Marr, J., Harff, P., Shanmugam, G., & Parker, G. (2001), Experiments on subaqueous sandy gravity flows: The role of clay and water content in flow dynamics and depositional structures. *Geological Society of America Bulletin* 113(11), pp. 1377.

Miura, N., S. Horpibulsuk, and T. S. Nagaraj. 2001. Engineering behavior of cement stabilized clay at high water content. *Soils and Foundations* 41 (5):33–45. doi:10.3208/sandf.41.5_33

Mohrig, D., Ellis, C., Parker, G., Whipple, K. X., & Hondzo, M. (1998). Hydroplaning of subaqueous debris flows. *Geological Society of America Bulletin*, 110(3), 387-394.

Mohrig, D., Elverhøi, A., & Parker, G. (1999). Experiments on the relative mobility of muddy subaqueous and subaerial debris flows, and their capacity to remobilize antecedent deposits. *Marine Geology*, 154(1), 117-129.

Mohrig, D., & Marr, J. G. (2003). Constraining the efficiency of turbidity current generation from submarine debris flows and slides using laboratory experiments. *Marine and Petroleum Geology*, 20(6), 883-899.

Rao, D. K., Raju, R. P., Sowjanya, C., & Rao, J. P. (2009). Laboratory studies on the properties of stabilized Marine Clay from Kakinada Sea Coast, India. *International Journal of Engineering Science and Technology*, 3(1), 422-428.

Taylor, R. N. _1995_. *Geotechnical centrifuge technology*, Blackie, Glasgow, U.K.

Wang, J. K. (2012). Monotonic and Cyclic Uplift Resistance of Buried Pipelines in Cohesionless Soils. *PhD thesis*, University of Cambridge, UK.

Wang, F., Dai, Z., & Zhang, S. (2017). Experimental study on the motion behavior and mechanism of submarine landslides. *Bulletin of Engineering Geology and the Environment*, 1-10.

Yin, M. and Y. Rui. 2017. Laboratory study on submarine debris flow. *Marine Georesources & Geotechnology*, 1–9

Figure 1. The Minidrum Centrifuge

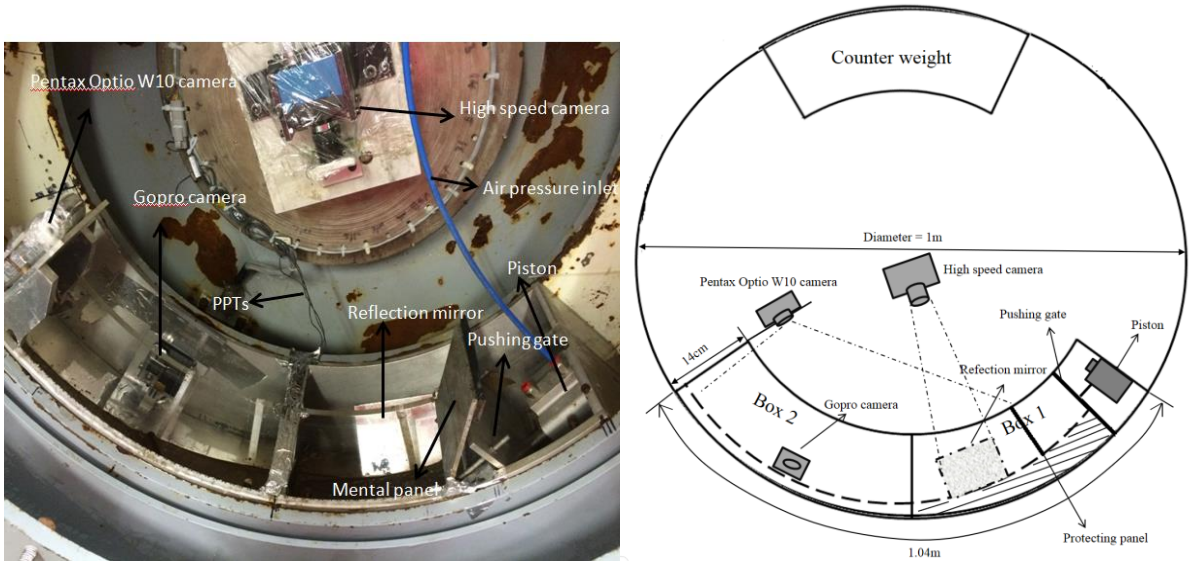

Figure 2. Experiment set-up

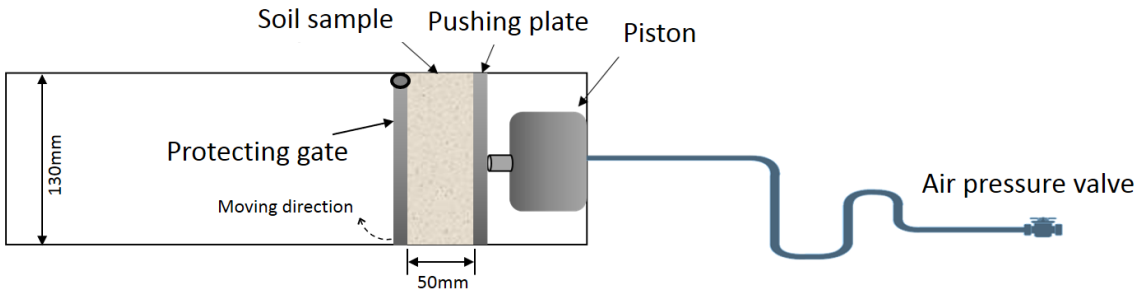

Figure 3. The schematic diagram of trigger system

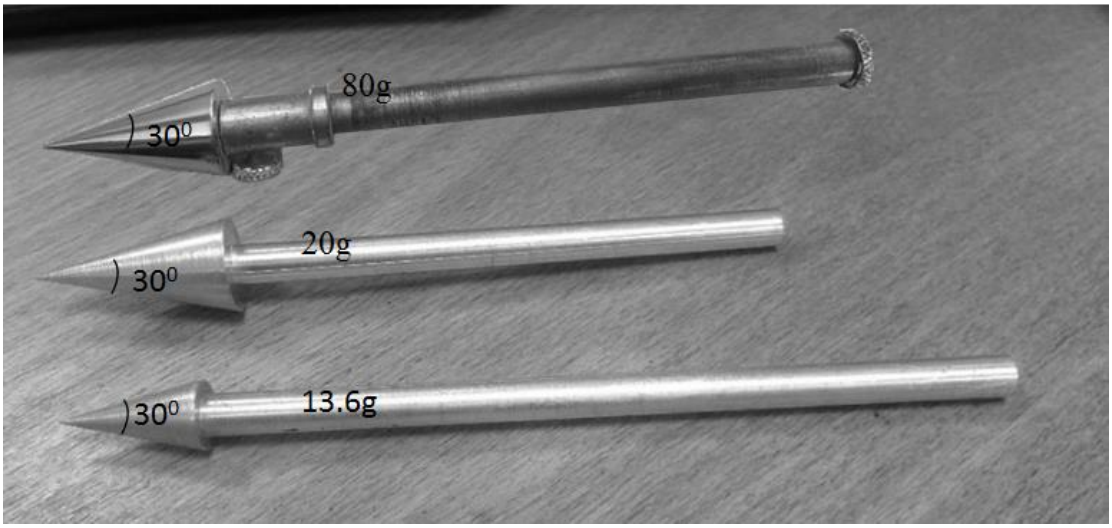

Figure 4. Three different cones used in the research

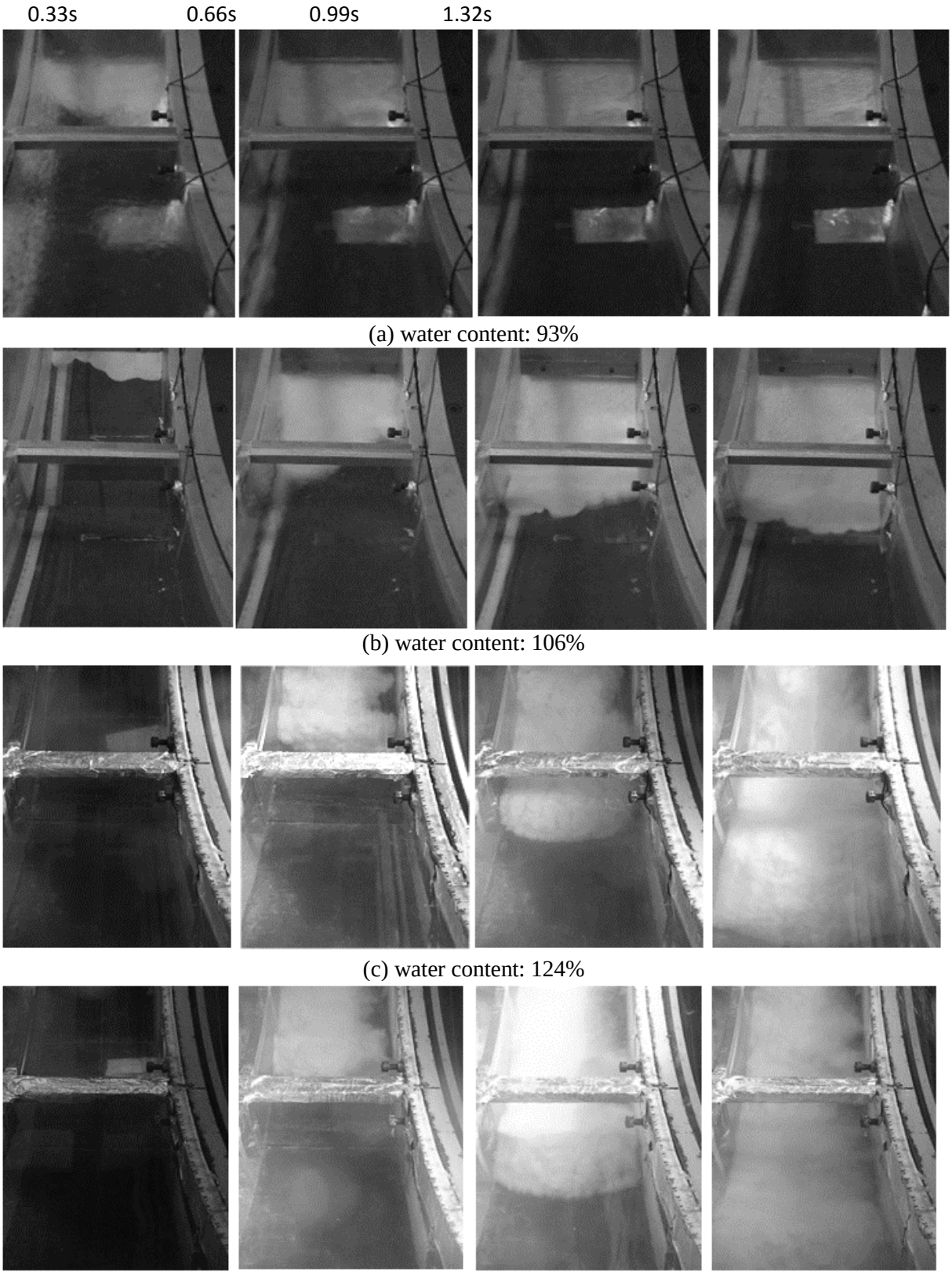

(a) water content: 93%

(b) water content: 106%

(c) water content: 124%

(d) water content: 133%

Figure 5. Plan view of the flow with different water content

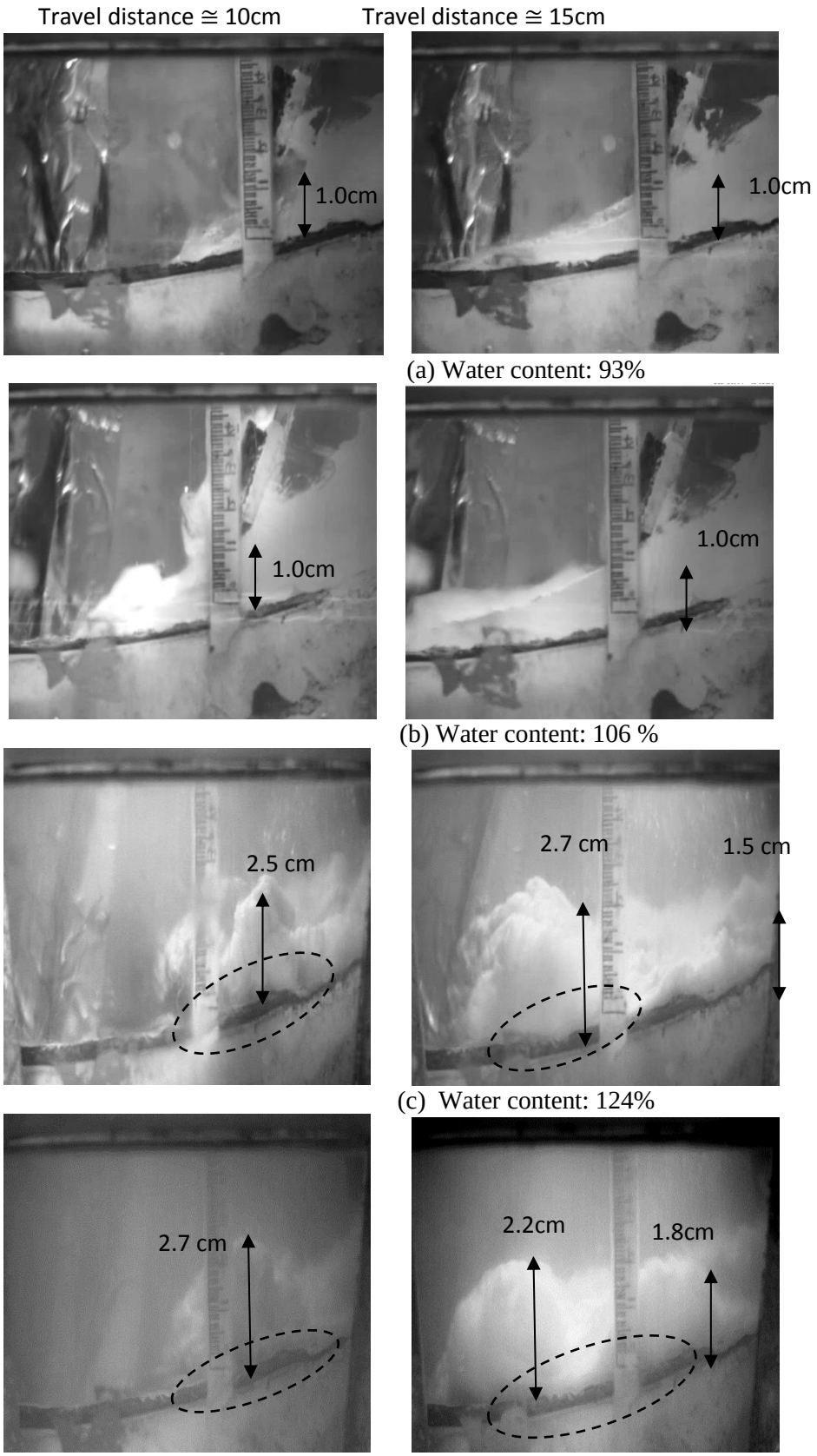

Figure 6. Side view of submarine landslide flows with various water contents

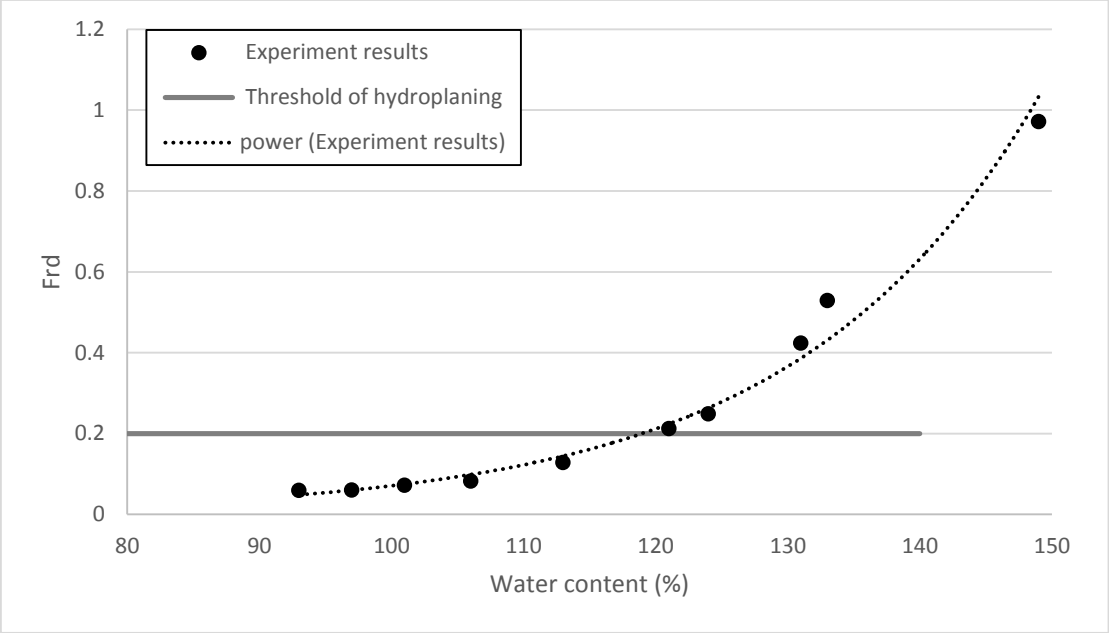

Figure 7. Values of the densimetric Froude number Fr_d

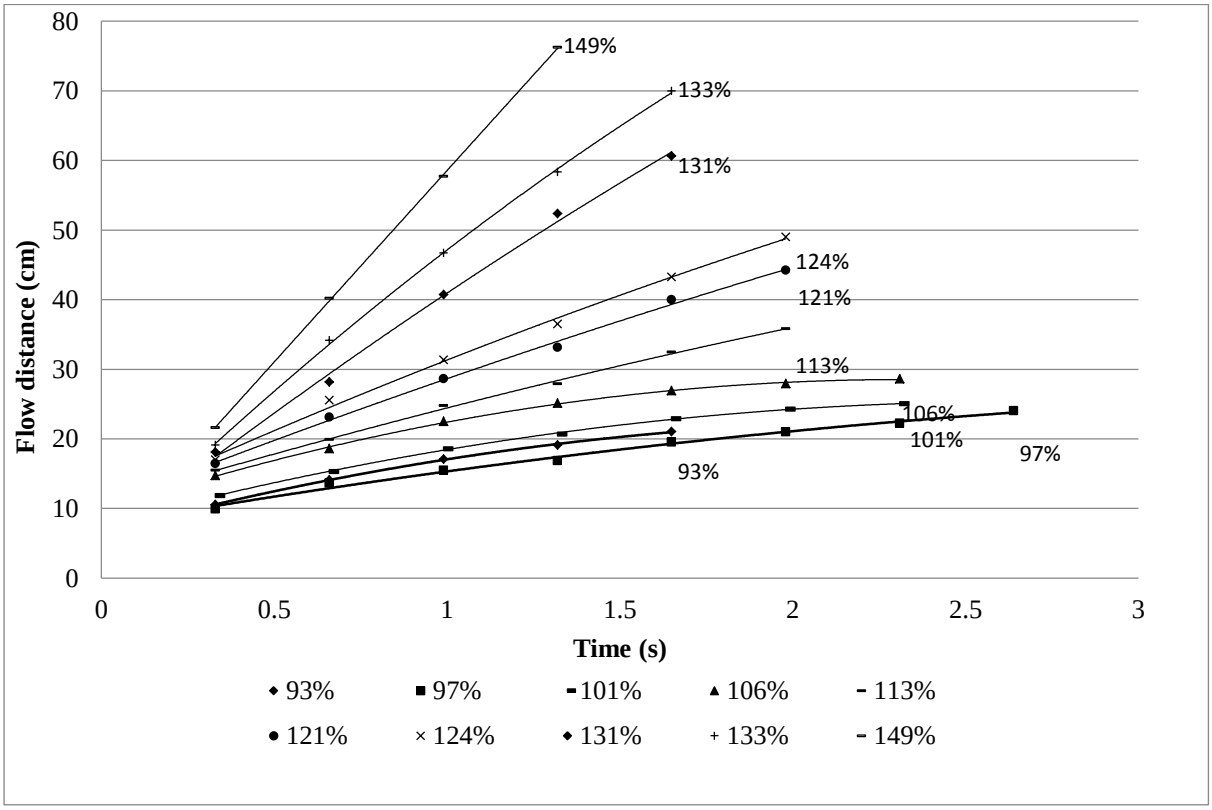

Figure 8. Flow distance against time for flows with various water contents

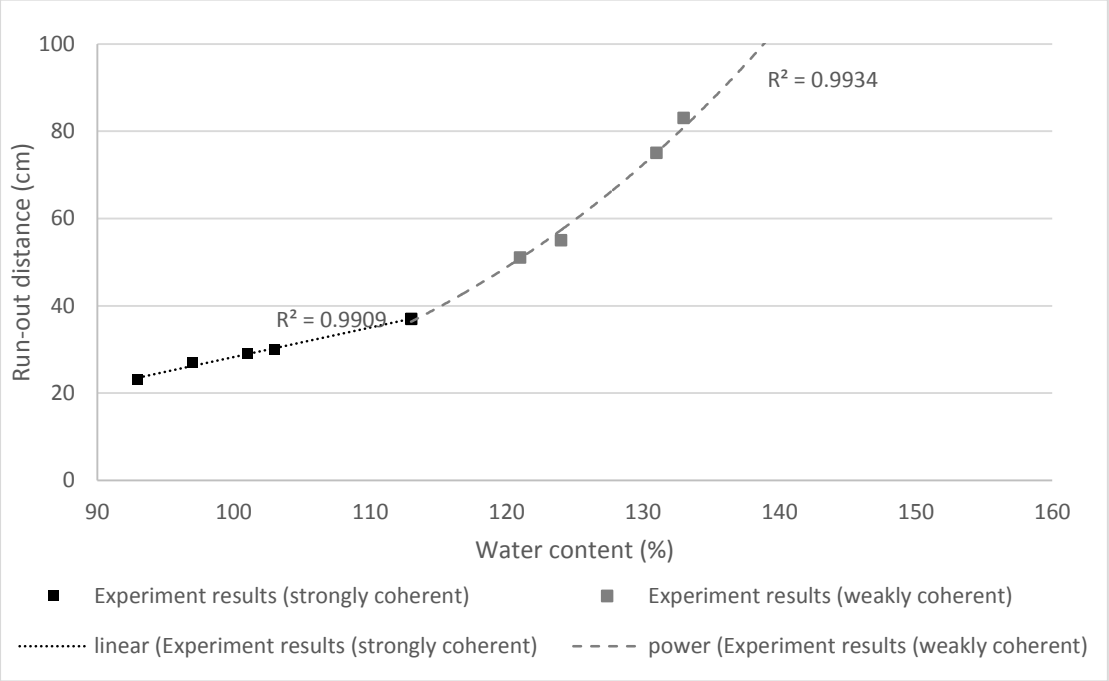

Figure 9. Relationship between flow initial water content (up to 133%) and flow distance

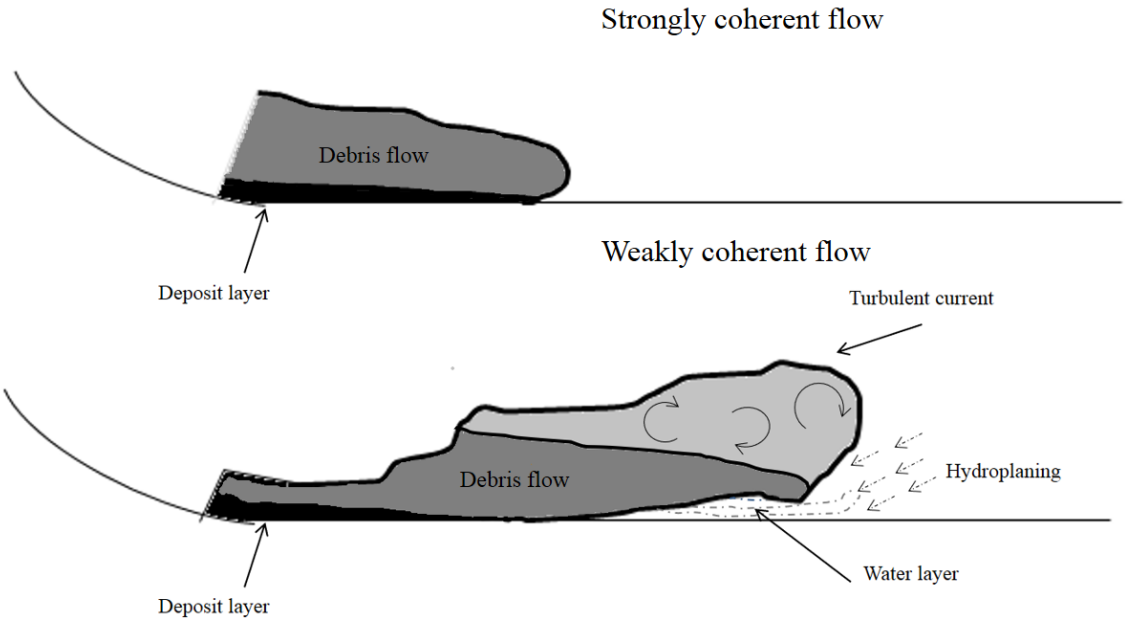

Figure 10. Mechanisms of high mobility of submarine debris flow

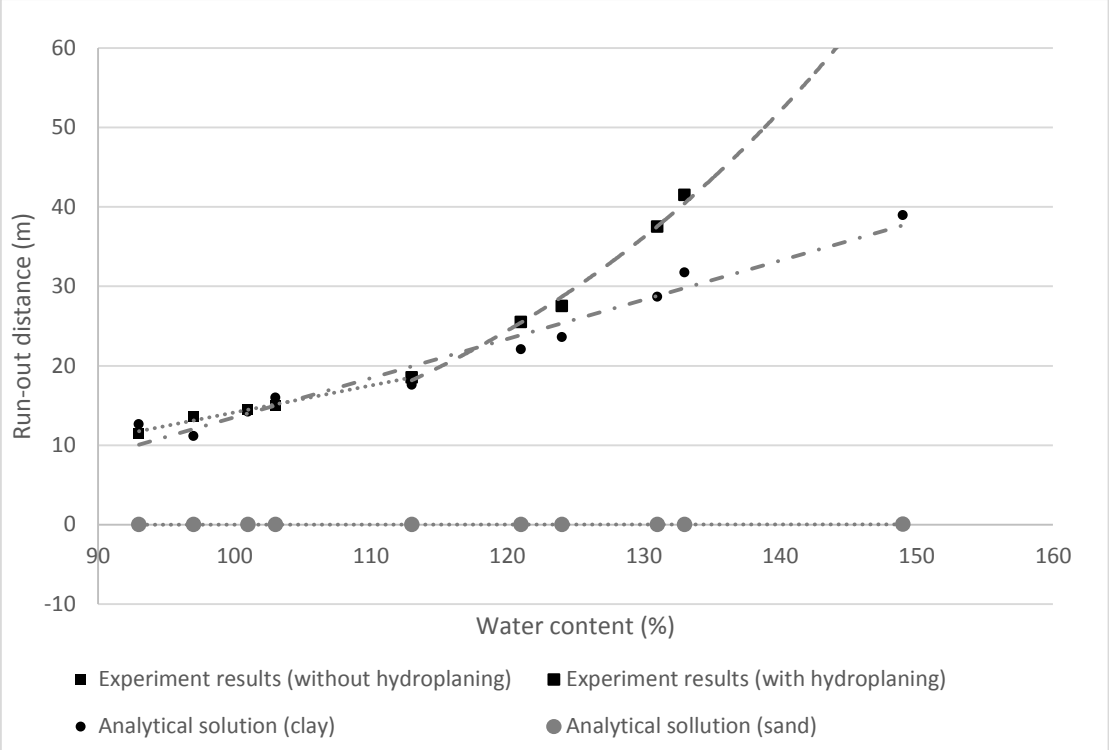

Figure 11. Calculated runout distance with varying water content